Temperature dependence of the density of aqueous alkali halide salt solutions by experiment and molecular simulation

Steffen Reiser, Martin Horsch,* and Hans Hasse

Laboratory of Engineering Thermodynamics, University of Kaiserslautern, 67653 Kaiserslautern, Germany

E-mail: martin.horsch@mv.uni-kl.de

Abstract

The density of aqueous alkali halide salt solutions is studied experimentally at 293.15, 303.15, 313.15, 323.15, and 333.15 K at 1 bar for solutions containing all soluble combinations of alkali cations (Li^+, Na^+, K^+, Rb^+, Cs^+) with halide anions (F^-, Cl^-, Br^-, I^-) at salt concentrations up to 0.05 mol/mol. The temperature dependence of the density of the electrolyte solutions is also determined by molecular simulation in the same temperature and composition range. The force fields of the ions are taken from previous work of our group [J. Chem. Phys. **136**, 084501 (2012), J. Chem. Phys. **140**, 044504 (2014)] and consist of one Lennard-Jones (LJ) site and a point charge. Water is modeled with the SPC/E force field. A very good agreement between the predictions from molecular simulation and the experimental data of the reduced density is found. In addition, the temperature dependence of the radial distribution function of water around the ions, the hydration number and the residence time of water molecules in the first hydration shell, the self-diffusion coefficient of the ions and the electric

*To whom correspondence should be addressed

conductivity is systematically studied by molecular simulation and compared to experimental literature data where available.

Keywords: aqueous electrolyte solutions, alkali halide salts, density measurements, molecular simulation

1. Introduction

Aqueous electrolyte solutions are of special importance in many natural and technical processes. One of the most fundamental thermodynamic properties of the electrolyte solutions is the density. In the temperature range studied in the present work (293.15 - 333.15 K) plenty of experimental density data for various aqueous alkali halide salt solutions are listed in databases.[1–5] However, to the best of our knowledge there is a lack of density data for less common electrolyte solutions, e.g. rubidium and cesium halide salt solutions for temperatures above 293.15 K. Density data for cesium halide salt solutions are generally only available in a narrow concentration range for temperatures above 313.15 K. For the rubidium halide salt solutions no density data are available at 333.15 K. In case of rubidium and cesium fluoride salt solutions experimental data are entirely missing above 293.15 K.

Several correlation methods[6] exist for the temperature dependence of the density of electrolyte solutions. They have many adjustable parameters that are fitted to experimental data and should only be used in the temperature and composition range of the data to which they were fitted.[6] There are only very few estimation methods for the density of electrolyte solution as a function of temperature and composition in the literature.[6] These methods[7,8] predict the density of the solution from the density of the pure solid salt and are known to yield rather inaccurate results.[6]

Molecular simulations of electrolyte solutions with classical force fields go far beyond these methods. In addition to the estimation of thermodynamic properties at arbitrary conditions, these simulations also provide a detailed insight into the structure and the processes in the solution at the molecular level. However, this requires accurate force fields both for the ions and the solvent. The

density, which is closely related to intermolecular distances, is vital for the validation of any kind of force fields. The prediction of the density of aqueous alkali halide salt solution as a function of temperature by molecular simulation is influenced by the accuracy both of the ion force field and the water model.

In recent years, many different force fields for the alkali cations and the halide anions have been developed.[9–22] Different parameterization strategies with different objectives were applied. The ion force fields were adjusted, e.g. to free energy data,[18,19,21] activity data[20,22] as well as data of the density of the solutions.[16] The strategies and the capability of the resulting ion force fields are discussed in more detail by Reiser et al.[23] and Moucka et al.[24] In recent work of our group, ion force fields for all alkali cations and halide anions were developed. They were adjusted to data of the density of the solutions, the self-diffusion coefficient of the ions in solution and the position of the first maximum of the radial distribution function of water around the ions.[23,25] These ion force fields consist of one Lennard-Jones (LJ) site and a concentric point charge with the magnitude of $\pm 1\ e$. The LJ size parameters were adjusted in a global fit to reduced densities of all aqueous alkali halide salt solutions at 293.15 K and 1 bar, whereas the LJ energy parameter, which has only a minor influence on the density,[25] was adjusted to the self-diffusion coefficient of the ions in solution in combination with the position of the first maximum of the radial distribution function of water around the ions at 293.15 K and 298.15 K, respectively, and 1 bar. The reduced density of the solution $\widetilde{\rho}$ is defined as

$$\widetilde{\rho} = \frac{\rho}{\rho_{\mathrm{W}}}\ , \tag{1}$$

where ρ is the density of the solution and ρ_{W} is the density of pure water at the same temperature and pressure. The reduced density was considered as objective rather than the density of the solution ρ to reduce the influence of the water model.[25] The resulting force fields for the alkali cations and halide anions reproduce the experimental reduced density of all soluble alkali halide salts solution over a wide composition range at 293.15 K and 1 bar well.[25] Moucka et al.[24] recently showed that, when the SPC/E force field[26] is used for water, the force fields for the sodium cation and the chloride anion from Deublein et al.[25] and the force fields of Smith and Dang[13] give the

best results for the density of relatively dilute aqueous NaCl solutions at 293.15K and 1 bar in comparison to other SPC/E compatible ion force fields from the literature. Using the SPC/E water model in combination with these ion force fields, the simulation results show a good agreement with the experimental self-diffusion coefficient data of the ions, the electric conductivity, the hydration dynamics of water molecules around the ions and the enthalpy of hydration at 293.15 K and 298.15 K, respectively, and 1 bar.[23]

The temperature dependence of thermodynamic properties of electrolyte solutions in the temperature range from 293.15 to 333.15 K was investigated in only a few studies in the literature by molecular simulation.[27–31] To the best of our knowledge, the temperature dependence of the density of electrolyte solutions was not yet studied by molecular simulation. Therefore, in the present work the temperature dependence of aqueous alkali halide salt solutions was studied comprehensively by molecular simulation with the force fields developed in previous work of our group.[23,25] However, for such a comparison the experimental density data from the literature had to be extended.

In the present study, density measurements of the aqueous electrolyte solutions of all soluble alkali halide salts were conducted (LiF is insoluble in water). Gaps in the existing literature data are filled and a systematic comprehensive data set on densities of solutions is provided. The density measurements were conducted for ion mole fractions of x_i = 0.01, 0.03 and 0.05 mol/mol at temperatures of 293.15, 303.15, 313.15, 323.15, and 333.15 K. Throughout this study all properties were investigated at 1 bar. The composition is given in terms of the ion mole fraction x_i, which is defined as

$$x_i = \frac{n_i}{2 \cdot n_i + n_\mathrm{W}} \,, \tag{2}$$

where n_i is the mole number of each ion type and n_W the mole number of water molecules in the electrolyte solution. For the 1:1 salt studied here, the ion mole fraction of the anions and the cations is x_i each. The ion mole fraction is related to the overall salt mole fraction

$$x_\mathrm{S} = \frac{n_\mathrm{S}}{n_\mathrm{S} + n_\mathrm{W}} \tag{3}$$

by

$$x_{\mathrm{S}} = \frac{x_i}{1 - x_i} \tag{4}$$

as the mole number of salt in the solution $n_{\mathrm{S}} = n_i$, regarding the salt as a single component. Molecular simulations at the same temperature, pressure and composition as in the experiments were carried out to determine the density of the electrolyte solutions. The accuracy of the predictions from molecular simulation for the reduced density of the solutions was assessed on the basis of the present experimental data. The simulation results and the experimental data are discussed individually for the different alkali halide salt solutions. Furthermore, the temperature dependence of structural, dynamic and transport properties of the electrolyte solutions was determined by molecular simulation. Water was modeled in this study with the SPC/E model,[26] which is one of the most commonly applied water force fields. It is widely used in biochemical research, and most force fields for biomolecules, like AMBER,[32] CHARMM[33] and GROMOS,[34] are based on SPC/E. Because the main component in the investigated electrolyte solutions is water, the simulation results are highly influenced by the accuracy of the SPC/E model. The temperature dependence of the density of pure liquid water at 1 bar is shown in Figure 1. The SPC/E model reproduces the experimental density of water well only at temperatures of around 298.15 K. Both with decreasing and increasing temperature, increasing deviations are observed. In the temperature range studied in the present work, the largest deviation is 0.7 % (at 333.15 K), cf. Figure 1.

In Section 2, the experiments are described. The employed force fields and the simulation methods are introduced in Section 3. In Section 4, the experimental data and the simulation results are presented and discussed. Section 5 concludes this work.

2. Experimental

Deionized water (produced by an Elix Essential 5^{UV} of Merck Millipore) was degassed by boiling before it was used for the preparation of the electrolyte solutions and the calibration of the den-

simeter. The reagent grade alkali halide salts were dried at 383 K in an oven for at least 24 h. The purity and the suppliers of the alkali halide salts are shown in Table 1. Samples of about 10 ml of electrolyte solutions with ion mole fractions of x_i = 0.01, 0.03, and 0.05 mol/mol were prepared gravimetrically (AE240, Mettler-Toledo). Considering the resolution of the balance and the error by determining the concentrations gravimetrically, the overall relative error in x_i is estimated by error propagation to be below ±0.1% for the investigated concentrations. The strongly hygroscopic salts (LiI, KF and CsF) were dried in a vacuum oven for 48 h and handled in a glove box in dry nitrogen atmosphere.

The density of the solution was determined with a vibrating tube densimeter (DMA 4500M, Anton Paar). The densimeter was initially calibrated with air and degassed, deionized liquid water. The measurements were carried out at temperatures of 293.15, 303.15, 313.15, 323.15, and 333.15 K. Based on the resolution of the densimeter and results from the repetition of experiments at the same conditions, the accuracy of the density measurements was found to be better than ±0.0001 g/cm^3. The accuracy of the temperature measurements are reported to be better than ±0.1 K.

3. Molecular simulation

In this study, rigid, non-polarizable force fields of the LJ type with one (ions) and three (water) superimposed point charges were used. For the unlike LJ parameters, the Lorentz-Berthelot[35,36] combining rules were employed. This choice was discussed in detail by Reiser et al.[23] An elaborate discussion of the available combining rules and their theoretical background is given by Schnabel et al.[37]

The LJ parameters of the alkali cations and halide anions were taken from preceding work of our group.[23,25] The LJ size parameters of the ion force fields are listed in Table 2. For the LJ energy parameter of the different ion force fields a unique value of $\varepsilon_i/k_\mathrm{B}$ = 200 K is used as recommended by Reiser et al.[23] Water was model in this study with the SPC/E[26] force field.

In the present study, the temperature dependence of the density as well as structural and dynamic properties of aqueous electrolyte solutions were determined by molecular simulation. The investigated structural and dynamic properties are: the radial distribution function (RDF) $g_{i\text{-O}}(r)$ of water around the ion i, the hydration number $n_{i\text{-O}}$ and the residence time $\tau_{i\text{-O}}$ of water molecules in the first hydration shell around the ion, the self-diffusion coefficient D_i of the ions and the electric conductivity σ of the solution. The methods for the determination of $g_{i\text{-O}}(r)$,[38] $n_{i\text{-O}}$[39] and $\tau_{i\text{-O}}$[40] are formally introduced in the literature. In the calculation and evaluation of these properties the position of the water molecules is represented by the position of the oxygen atom.

Following a proposal by Impey et al.[27] for the calculation of the residence time $\tau_{i\text{-O}}$, unpairing of an ion and a water molecule was assumed if their separation lasted longer than the residence time $\tau_{\text{O-O}}$ of a water molecule around a neighboring molecule in a pure bulk water simulation at the same conditions. However, a short-time pairing of two particles $\tau_{i\text{-O}} < \tau_{\text{O-O}}$ was fully accounted for in the calculation $\tau_{i\text{-O}}$.

The self-diffusion coefficient of the ions and the electric conductivity of the aqueous solutions were determined via equilibrium molecular dynamics (MD) simulations by means of the Green-Kubo formalism.[41,42] This formalism establishes a direct relationship between a transport coefficient and the time integral of the autocorrelation function of the corresponding flux within a fluid. The Green-Kubo expression for the self-diffusion coefficient D_i is based on the individual ion velocity autocorrelation function[43] and the electric conductivity σ is related to the autocorrelation function of the electric current flux $\boldsymbol{j}(t)$. The electric current autocorrelation function may be decomposed[44] into an autocorrelation function $Z(t)$ and a crosscorrelation function $\Delta(t)$ that quantifies the deviation from ideal Nernst-Einstein behavior.[39,44] The meaning of the terms $Z(t)$ and $\Delta(t)$ is described in detail by Reiser et al.[23]

In this work, an extended version of the molecular simulation program *ms2*[45] was used. Technical details are given in the Appendix: Simulation details.

4. Results and discussion

4.1 Experimental data

The experimental data of the density of aqueous alkali halide solutions as well as that of pure liquid water determined in the present work is given in Table 3. The present experimental data at 293.15 K are in excellent agreement with literature data[1–3] over the entire investigated composition range. The deviations are always below 0.1 % except for NaBr and NaI where the deviations for some data points are up to 0.13 % and 0.18 %, respectively. The agreement with the literature data is also good for temperatures above 298.15 K. Where comparison is possible, the deviations are below 0.1 %. Exemplarily, the present experimental density data of all investigated alkali bromide salt solutions are compared to literature data[1–3] in Figure 2.

The density ρ of all studied electrolyte solutions increases linearly as a function of the ion mole fraction x_i at a given temperature in the concentration range studied in the present work (cf. Figure 2 and Table 3). The corresponding data of the slope a of ρ over x_i with

$$\rho = \rho_{\mathrm{W}} + a \cdot x_i \tag{5}$$

at 293.15 and 333.15 K are listed in Table 4. For all lithium, sodium and potassium halide salts the standard deviation of the correlation for the density of the aqueous electrolyte solutions (Eq. (5)) is better than ±0.001 g/cm^3 and for the rubidium and cesium halide salts better than ±0.003 g/cm^3. Exceptional cases are the solutions of KI with a standard deviation of ±0.003 g/cm^3, of RbI with ±0.004 g/cm^3 and of CsI with ±0.006 g/cm^3. The slope a is individual for the different alkali halide solutions but, in the investigated temperature range, almost independent on the temperature (cf. Table 4). The density of the electrolyte solutions decreases with increasing temperature. This decrease is for all alkali halide salt solutions at all investigated concentrations nearly identical to the decrease of the density of pure liquid water with increasing temperature. Hence, the reduced density $\widetilde{\rho}$ of the electrolyte solutions is almost independent on the temperature. A discussion of the

overall partial molar volume of the electrolyte solutions is given in the Appendix: Partial molar volume.

4.2 Comparison of simulation results and experimental data

The simulation results of the density ρ of the alkali halide salt solutions as well as pure liquid water are listed in Table 5.

In the present simulation study, the prediction of the temperature independence of the slope a of ρ over x_i and consequently of the reduced density $\widetilde{\rho}$ by the ion force fields is investigated in particular. The simulation results of the slope a are compared to experimental data at 293.15 and 333.15 K in Figure 3. The independence of the experimental data of a on the temperature is predicted well by the molecular simulations. The discontinuous increase of a with increasing coordination number of the ions (e.g. identical slopes a for sodium and potassium halide salt solutions) can be attributed to a superposition of the increasing ion size, the increasing ion mass and the influence of the ion on the structure of the surrounding hydrogen bonding network of the water molecules. The discussion of the effect of structure making and breaking by ions in aqueous solution is beyond the scope of this work and can be found in the literature, e.g. in Mähler and Persson.[46] The comparison between simulation results and experimental data of the reduced density $\widetilde{\rho}$ of alkali fluoride and chloride salt solutions is shown in Figure 4, and for alkali bromide and iodide salt solutions in Figure 5. Analogous to the experimental data, the simulation results of $\widetilde{\rho}$ at 293.15 and 333.15 K are found to be almost identical in all cases. Figures 3, 4 and 5 also reveal that the modification by Reiser et al.[23] of the LJ energy parameter ϵ of the ion force fields from Deublein et al.[25] has no significant influence on the reduced solution density. The dependence of the simulation results of the reduced density $\widetilde{\rho}$ of the different alkali halide salt solutions on the concentration and the comparison to experimental data at 293.15 K was discussed previously by Deublein et al.[25]

4.3 Structural properties

The temperature dependence of the RDF $g_{i-\mathrm{O}}(r)$ of water around the alkali cations and halide anions in aqueous solution was determined by molecular simulation in the temperature range from 293.15 to 333.15 K. The simulations were conducted at an ion mole fraction of x_i = 0.01 mol/mol, i.e. at low salinity. Hence, the results of $g_{i-\mathrm{O}}(r)$ around the single ions are almost independent on the chosen counterion in solution. The RDF of water around the ions was determined for LiCl, NaBr, KF, RbI and CsCl salt solutions.

The temperature dependence of the RDF of water around the ions in the temperature range from 293.15 to 333.15 K is listed in numerical form in Table 6 and is shown exemplarily for iodide in Figure 6. The stronger thermal motions of the water molecules with increasing temperature lead to a slight decline of the structuring in the hydration shell. Hence, the RDF $g_{i-\mathrm{O}}(r)$ slightly decreases at the first and second maximum and increases at the first minimum.[28] At the same time, the distances of the first minimum and second maximum slightly increase with increasing temperature, cf. Figure 6 and Table 6. However, the position of the first maximum $r_{\mathrm{max},1}$ is independent on temperature[27,28] for all ions in the investigated temperature range, cf. Table 6. These facts were also observed in simulation studies in the literature.[27–29] The temperature dependence of the RDF varies for the different ions and is individually discussed for the cations and anions in the following. The dependence of $g_{i-\mathrm{O}}(r)$ on the size and the sign of the ions at 293.15 K was discussed earlier by Reiser et al.[23]

Alkali cations: In case of Li^+ and Na^+, the distance $r_{\mathrm{min},1}$ is constant in the investigated temperature range, whereas $r_{\mathrm{max},2}$ is slightly shifted to larger distances. For K^+, Rb^+ and Cs^+ the temperature induced shift of both $r_{\mathrm{min},1}$ and $r_{\mathrm{max},1}$ increases with increasing ion size, cf. Table 6. Larger ions possess a weaker bonded hydration shell[23] and hence the influence of the accelerated thermal motions on the positions of the first minimum and second maximum of the RDF is more pronounced. For $g(r_{\mathrm{max},1})$ and $g(r_{\mathrm{max},2})$ a decline of the temperature dependence with increasing ion size is observed, cf. Table 6. In comparison to small cations, the orientation of the water molecules around larger cations is less directed and lower values of the maxima of $g_{i-\mathrm{O}}(r)$ are found.[23] Hence, the

influence of accelerated thermal motions of the water molecules around cations on the maxima of the RDF is more pronounced for smaller ions. The influence of the temperature on $g(r_{\mathrm{min},1})$ is very low for all cations. In case of Li^+ and Na^+, this can be attributed to the highly structured first hydration shell with $g(r_{\mathrm{min},1}) \approx 0$, whereas the weaker structure of the water molecules around ions with less pronounced extremes of $g_{i-\mathrm{O}}(r)$ is the reason for the weak temperature dependence of $g(r_{\mathrm{min},1})$ in case of larger cations.

Halide anions: The highly structured and strongly bonded hydration shell around the anions leads to a small shift of the position $r_{\mathrm{min},1}$ (> 0.06 Å) within the investigated temperature range as well as to the temperature independence of $r_{\mathrm{max},2}$ for all anions, cf. Table 6. The influence of the temperature on the extremal values of $g_{i-\mathrm{O}}(r)$ around F^- is, although the ions possess almost the same size, significantly more pronounced than around the cesium cation, cf. Table 6. This is attributed to the more structured and stronger bonded hydration shell around the fluoride anion.[23] A weaker influence of the temperature on $g(r_{\mathrm{max},1})$, $g(r_{\mathrm{min},1})$, and $g(r_{\mathrm{max},2})$ with increasing anion size was observed (cf. Table 6), which can be attributed to the increasingly weaker structure of the water molecules around the anions.

4.4 Hydration number

The temperature dependence of the hydration number $n_{i-\mathrm{O}}$ in the first hydration shell around the ions was evaluated in the temperature range from 293.15 to 333.15 K. The basis of the calculations of $n_{i-\mathrm{O}}$ are the RDF $g_{i-\mathrm{O}}(r)$ from the previous section. Hence, the results of $n_{i-\mathrm{O}}$ are almost independent on the counterion in the solution.

The hydration number $n_{i-\mathrm{O}}$ in the first hydration shell around the different cations and anions is shown in Table 7. The dependence of the hydration number on the different ions was discussed earlier by Deublein et al.[25] In case of all ions, the simulation results of $n_{i-\mathrm{O}}$ are independent on the temperature. The effects of the temperature on $g_{i-\mathrm{O}}(r)$ in the first hydration shell, i.e. the reduction of $g(r_{\mathrm{max},1})$ and the increase of $g(r_{\mathrm{min},1})$ with increasing temperature (cf. Section 4.3),

cancel out in the calculation of $n_{i-\mathrm{O}}$. Hence, even though the mobility of the water molecules in the first hydration shell increases with increasing temperature their total number is constant. This finding is consistent with the results from the simulation studies on the temperature dependence of $n_{i-\mathrm{O}}$ from Reddy and Berkowitz[28] and Zavitsas.[30] There, a reduction of $n_{i-\mathrm{O}}$ with increasing temperature was observed only in a considerably wider temperature range.

4.5 Hydration dynamics

The temperature dependence of the residence time $\tau_{i-\mathrm{O}}$ of water molecules around the ions was determined by MD simulation in the temperature range from 293.15 to 333.15 K. The residence time was sampled for the same aqueous electrolyte solutions and under the same conditions as the RDF $g_{i-\mathrm{O}}(r)$, c.f. Section 4.3. Again, the results of $\tau_{i-\mathrm{O}}$ are almost independent on the counterion in the electrolyte solution.

The residence time of water molecules $\tau_{i-\mathrm{O}}$ around the different cations and anions as well as in pure liquid water $\tau_{\mathrm{O-O}}$ at different temperatures is shown in Figures 7 and 8, respectively, and is listed in numerical form in Table 8. The present simulation results of $\tau_{\mathrm{Li-O}}$ are similar to data published by Egorov et al.[29] For a given temperature, the residence time $\tau_{i-\mathrm{O}}$ around each ion is longer than $\tau_{\mathrm{O-O}}$, which is attributed to the stronger electrostatic attraction between the ion and the surrounding water molecules. The dependence of the residence time on the size and the sign of the ions at 293.15 K was discussed earlier by Reiser et al.[23]

Accelerated thermal motion of the molecules with increasing temperature leads to shorter residence times both for $\tau_{\mathrm{O-O}}$ and $\tau_{i-\mathrm{O}}$. The decline of the residence time with increasing temperature is almost linear in the investigated temperature range. The same trend was also observed for $\tau_{\mathrm{Li-O}}$ in the simulation study by Egorov et al.[29] However, the slope of the residence time over the temperature is individual for the different ions as well as for pure liquid water, cf. Figures 7 and 8 and Table 8. In case of the alkali cations and the halide anions, the largest decline of the residence time over the temperature was found for $\tau_{\mathrm{Li-O}}$ and $\tau_{\mathrm{F-O}}$, respectively. With increasing size

of both cations and anions, and hence decreasing electrostatic attraction between the ions and the surrounding water molecules, the decline of $\tau_{i-\mathrm{O}}$ over the temperature decreases. Thus, the temperature dependence of the residence time is more pronounced for stronger bonded hydration shells. However, the absolute values of the residence time $\tau_{\mathrm{Li-O}}$ and $\tau_{\mathrm{F-O}}$ are significantly longer than for other cations and anions, respectively, even at the highest investigated temperature 333.15 K. The lowest dependence on the temperature was observed in this study for $\tau_{\mathrm{O-O}}$.

4.6 Self-diffusion coefficient

The temperature dependence of the self-diffusion coefficient of pure liquid water D_{W} as well as of the alkali cations and halide anions in aqueous solution was investigated in the temperature range from 293.15 to 333.15 K. The ion self-diffusion coefficient D_i was determined at low salinity (x_i = 0.009 mol/mol). Hence, the influence of correlated motions between anion and cation in the solution is low and D_i is almost independent on the counterion type.

Because the ions move through the solution together with their hydration shell,[23] their mobility is dominated both by the effective radius of this ion-water complex and the mobility of the surrounding bulk water molecules. Hence, the temperature dependence of the ion mobility is directly linked to the temperature dependence of the mobility of the bulk water molecules. The temperature dependence of the self-diffusion coefficient of pure liquid water, which is a measure for the mobility of the water molecules, is shown in Figure 9 and listed in numerical form in Table 9. With increasing temperature, accelerated thermal motions of the water molecules lead to more molecular mobility. The predictions from molecular simulation with the SPC/E water model[26] follow the qualitative trend measured by experiments.[47–52] However, the simulation results overestimate the self-diffusion coefficient of pure liquid water in the investigated temperature range. The deviations decrease with increasing temperature from 18 % at 293.15 K to 3 % at 333.15 K. This decline of the deviations with increasing temperature was reported in the literature.[31,53]

The temperature dependence of the self-diffusion coefficient of the ions in aqueous solution in comparison to D_{W} of pure liquid water is shown in Figure 10 for the alkali cations and in Figure 11 for the halide anions and is listed in numerical form in Table 9. The self-diffusion coefficient of the ions D_i increases with increasing temperature. The mobility of the ions is highly influenced by the mobility of the water molecules, but the temperature dependence is not identical for pure liquid water and the ions in aqueous solution. Furthermore, the temperature dependence varies for the different ions. Unfortunately, experimental data for the self-diffusion coefficient of the alkali cations and halide anions are only available at 298.15 K within the investigated temperature range. [31] A comparison between simulation results and experimental data like in Figure 9 is hence not feasible. At 298.15 K, the overall agreement between the simulation results and the experimental data[54] is excellent.[23] The dependence of D_i on the size and the sign of the ions at 298.15 K was discussed earlier by Reiser et al.[54]

Alkali cations: From Li^+ to Rb^+, i.e. with increasing ion size, the self-diffusion coefficient D_i becomes more temperature dependent, cf. Figure 10 and Table 9. This effect was also observed for D_{Na} and D_{K} in a simulation study by Bastug et al.[31] With increasing ion size, the electrostatic attraction within the ion-water complex and hence the effective radius decreases,[23] i.e. the increase of the mobility at higher temperatures is more pronounced for smaller complexes. Hence, the varying temperature dependence of D_i is attributed to the different strength of the ion-water complexes and the resultant effective complex radii. An exception is the transition from Rb^+ to Cs^+. For larger ions, the effective radius of the ion-water complex is increasingly influenced by the ion diameter. Because of these opposing effects, the effective radius increases and the self-diffusion coefficient D_i decreases from Rb^+ to Cs^+. This can be seen both from experimental data[54] for D_{Rb} and D_{Cs} as well as from simulation results[23,40,55,56] at 298.15 K. Because of the smaller effective radius of the ion-water complex, the self-diffusion coefficient D_{Rb} is more temperature dependent than D_{Cs}, cf. Figure 10 and Table 9.

Halide anions: The weakest temperature dependence of D_i in case of the halide anions was observed for F^-. The fluoride anion has the strongest electrostatic attraction with respect to the water

molecules in the hydration shell and possesses the largest effective radius of the ion-water complex of all investigated anions.[23] In case of the other investigated anions, namely Cl^-, Br^- and I^-, the temperature dependence of D_i is very similar, cf. Figure 11 and Table 9. For these ions, the strength of the interaction between the ion and the water molecules in the hydration shell is similar[23] and there is only a minor relative increase due to the ion diameter. Hence, the effective radius of the ion-water complex of these ions is almost identical.

4.7 Electric conductivity

The temperature dependence of the electric conductivity σ of aqueous NaCl salt solutions was investigated for ion mole fractions up to $x_i = 0.018$ mol/mol in the temperature range from 293.15 to 333.15 K. This specific salt was chosen, because sufficient experimental data[3] over the entire investigated temperature range were available. The electric conductivity σ of additional aqueous alkali halide salt solutions was not in the scope of this study, since the simulation of σ is exceedingly computing time consuming, cf. Appendix: Simulation details.

In Figure 12 the simulation results of the electric conductivity σ of aqueous NaCl salt solutions at different temperatures and compositions are compared to experimental data.[3] The electric conductivity σ predicted at 293.15 K is in excellent agreement with the experimental data.[3] The deviations are below 6 % over the entire concentration range. The dependence of σ on the salt concentration at constant temperature was discussed earlier by Reiser et al.[23] The increase of the electric conductivity with increasing temperature is predicted by the simulation, but the deviation between the experimental data[3] and the simulation results increase. The maximum deviation at 333.15 K is 17 % for an ion mole fraction of $x_i = 0.018$ mol/mol. The electric conductivity of the aqueous NaCl salt solution is increasingly underestimated with increasing temperature over the entire investigated composition range, i.e. from high dilution up to an ion mole fraction of $x_i = 0.018$ mol/mol. This indicates that the deviations from the experimental data at higher temperatures are dominated by an increasing mismatch in the prediction of the mobility and hence the self-diffusion coefficient

of the ions by the present molecular simulations. As discussed in Section 4.6, the temperature dependence of the ion mobility is directly linked to the temperature dependence of the mobility of the surrounding bulk water molecules. The combination of the ion force fields and the SPC/E water model, which overestimates the self-diffusion coefficient D_{W}, leads at 293.15 K to an excellent agreement between simulation results and experiment data of σ of NaCl salt solutions up to x_i = 0.018 mol/mol. With increasing temperature, the mismatch of the water self-diffusion coefficient D_{W} due to the SPC/E model decreases, cf. Figure 9. The dependence of the self-diffusion coefficient of pure bulk water on the temperature is underestimated by the SPC/E model. Hence, the mobility of the ions and, accordingly, the electric conductivity was also increasingly underestimated with increasing temperature.

Further information on the temperature dependence of the microscopic electrolyte solution dynamics can be obtained by analyzing the particle trajectories. Therefore, the electric current time correlation function was separated into its two contributions, i.e. the autocorrelation term $Z(t)$ and the crosscorrelation term $\Delta(t)$. This analysis was carried out for an aqueous NaCl salt solution with an ion mole fraction of x_i =0.018 mol/mol at 293.15 and 333.15 K. The results for $Z(t)$ and $\Delta(t)$ for the two temperatures are shown in Figure 13. A more detailed general discussion of $Z(t)$ and $\Delta(t)$ is given by Reiser et al.[23]

The present analysis reveals that $\Delta(t)$, which describes the correlated motion of the ions, is nearly independent on temperature. At 333.15 K, correlated motions of oppositely charged ions ($\Delta(t) < 0$) were observed for short times < 0.30 ps, whereas the time span of negative $\Delta(t)$ at 293.15 K is only slightly shorter (< 0.26 ps). Hence, a significant increase of the temperature does not lead to more correlated motions of oppositely charged ions at this salt concentration. For longer times, the electric conductivity is dominated by the mobility and hence the self-diffusion of the single ions $Z(t)$. Unlike the crosscorrelation term $\Delta(t)$, the autocorrelation term $Z(t)$ highly depends on the temperature. The shift of $Z(t)$ up to higher values in the time span from $0 < t <$ 0.35 ps and the smoother rise of $Z(t)$ for $t >$ 0.35 ps with increasing temperature are attributed to the higher mobility of the sodium cations and chloride anions in the aqueous electrolyte solutions.

The extremes of $Z(t)$ and $\Delta(t)$ appear for both temperatures at nearly the same times. These oscillations are attributed to the permanent thermal vibrations of the ions within their hydration shell. Moreover, because the dependence of the solution structure on the temperature is weak, cf. Section 4.3, the same behavior was observed for all extremes of $Z(t)$ and $\Delta(t)$.

5. Conclusions

The temperature dependence of the density of all aqueous alkali halide salt solutions was determined both by experiment and molecular simulation from 293.15 to 333.15 K at 1 bar at ion mole fractions up to 0.05 mol/mol. Moreover, the influence of the temperature on the radial distribution function of water around the ions, the hydration number and residence time of water molecules in the first hydration shell around the ions, the self-diffusion coefficient of the ions and the electric conductivity was investigated by molecular simulation.

The density measurement results of the aqueous alkali halide salt solutions are in excellent agreement with data from the literature. Prior to this work, there was a lack of experimental density data of rubidium and cesium halide salt solutions for temperatures above 293.15 K. The simulation results of the slope a and of the reduced density $\widetilde{\rho}$ are in good agreement with the experimental data for all alkali halide salt solutions. The experimental data of a and $\widetilde{\rho}$ are found to be almost independent on the temperature, which is predicted correctly by the simulation results.

The structure of the water molecules in the first hydration shell changes with increasing temperature, but the hydration number is found to be constant in the investigated temperature range. The simulation results for the residence time of water molecules around the ions at different temperatures reveal that the reduction of $\tau_{i-\mathrm{O}}$ due to increasing thermal motion of the molecules at higher temperatures is larger for ions with stronger bonded hydration shells which generally exhibit longer absolute residence times.

The temperature dependence of the self-diffusion coefficient of the ions D_i determined by molec-

ular simulation is found to be individual for the ions. The increase of D_i with the temperature depends on the effective radius of the ion-water complex. Its size is affected both by the strength of the electrostatic interaction between the ion and the water molecules in the hydration shell and the diameter of the ion. The temperature dependence of the electric conductivity of aqueous NaCl salt solutions was predicted by molecular simulation. The simulation results are in good agreement with the experimental data. However, the deviation between the simulation and experiment increases with increasing temperature. This can be attributed to an increasing underestimation of the self-diffusion coefficients of Na^+ and Cl^- by the force fields.

Acknowledgments

The authors gratefully acknowledge financial support by DFG's Reinhart Koselleck Program as well as computational support by the Regionales Hochschulrechenzentrum Kaiserslautern (RHRK) under the grant MSWS and the High Performance Computing Center Stuttgart (HLRS) under the grant MMHBF2. The present research was conducted under the auspices of the Boltzmann-Zuse Society of Computational Molecular Engineering (BZS). We thank Jadran Vrabec, University of Paderborn, for fruitful discussions.

Appendix: Simulation details

For all simulations of this study, an extended version of the simulation program *ms*2[45] was employed. In *ms*2, thermophysical properties can be determined for rigid molecular models using Monte-Carlo (MC) or molecular dynamics (MD) simulation techniques. For all simulations, the LJ interaction partners are determined for every time step and MC loop, respectively. Interaction energies between molecules and/or ions are determined explicitly for distances smaller than the cut-off radius r_c. The simulation uncertainties were estimated with the block average method by Flyvberg and Petersen.[57]

The liquid density of aqueous alkali halide solutions was determined with the MC technique in the isothermal-isobaric ensemble at a constant pressure of 1 bar for different temperatures and compositions. Depending on the composition, the simulation volume contained 10, 30, or 50 cations. The total molecule number $N = 1000$ was constant in all simulations. A physically reasonable configuration was obtained after $5,000$ equilibration loops in the NVT ensemble , followed by $80,000$ relaxation loops in the NpT ensemble. Thermodynamic averages were obtained by sampling $512,000$ loops. Each loop consisted of $N_{\mathrm{NDF}}/3$ steps, where N_{NDF} indicates the total number of mechanical degrees of freedom of the system. Electrostatic long range contributions were considered by Ewald summation[58] with a real space convergence parameter $\kappa = 5.6$. The real space cut-off radius was equal to the LJ cut-off radius of 15 Å.

For the calculation of structural and dynamic properties of the aqueous electrolyte solutions, MD simulations were carried out. In a first step, the density of the aqueous alkali halide solution was determined by an NpT simulation at the desired temperature, pressure and composition. Subsequently, the self-diffusion coefficient, the electric conductivity, the radial distribution function and the residence time were calculated in the NVT ensemble at the same temperature and composition with the density resulting from the first step. In these MD simulations, Newton‘s equations of motion were solved with a Gear predictor-corrector scheme of fifth order with a time step of 1.2 fs. The long-range interactions were considered by Ewald summation.[58]

The self-diffusion coefficient of the ions[43] and the electric conductivity of the solution[59] were calculated with the Green-Kubo formalism.[41,42] For simulations in the NpT ensemble, a physically reasonable configuration was attained by $10,000$ time steps in the NVT ensemble and $100,000$ time steps in the NpT ensemble, followed by a production run over $800,000$ time steps. In the NVT ensemble, the equilibration was carried out over $100,000$ time steps, followed by a production run of $2,400,000$ time steps for the calculation of the self-diffusion coefficient and the electric conductivity. The sampling length of the velocity and the electric current autocorrelation functions was set to 11 ps and the separation between the origins of two autocorrelation functions was 0.2 ps. Within the separation time span, all correlation functions decayed to less than 1/e

of their normalized value. The MD unit cell with periodic boundary conditions contained 4500 molecules. This relative high number of molecules was used here to minimize the influence of the finite size effect on the simulation results. Using the Green-Kubo formalism[41,42] for the calculation of transport properties of aqueous systems, Guevara et al.[53] showed that the finite site effect saturates with increasing number of molecules. No significant differences were observed above 2048 molecules.[53] For the calculation of the self-diffusion coefficient, the simulation volume contained 4420 water molecules, 40 alkali ions and 40 halide ions. The electric conductivity was determined for different compositions. Hence, the number of ions in the simulation volume varied from 16 to 160. The real space and LJ cut-off radius was set to 25 Å.

The radial distribution function and the residence time were determined by molecular simulation of systems containing 10 cations, 10 anions and 980 water molecules. For simulations in the NpT ensemble, the system was equilibrated over $10,000$ time steps in the NVT ensemble and $100,000$ time steps in the NpT ensemble, followed by a production run over $1,000,000$ time steps. The RDF of water around the ions was sampled in the subsequent NVT ensemble simulation up to a cut-off radius of 15 Å with 500 bins. The results for the position of the first minimum of the RDF were used in a second NVT ensemble simulation with the same density for the determination of the residence time of water molecules around the ions. In both NVT simulations, the system was equilibrated over $100,000$ time steps, followed by a production run of $1,000,000$ time steps.

The same process was applied for the calculation of the pure water properties, i.e. the self-diffusion coefficient and the residence time of water molecules around their neighbors.

Appendix: Partial molar volume

The volume V of the electrolyte solutions is given by

$$V = n_{\mathrm{W}} \cdot v_{\mathrm{W}} + v_{\mathrm{S}} \cdot n_{\mathrm{S}} \,, \tag{6}$$

where n_{S} and n_{W} is the number of salt and water molecules, respectively, and v_{S} and v_{W} the overall partial molar volume of the salt and of water in the solution, respectively. The overall partial molar volume of the salt v_{S} in the aqueous solutions is defined as

$$v_{\mathrm{S}} = \left(\frac{\partial V}{\partial n_{\mathrm{S}}} \right)_{T,p,n_{\mathrm{W}}} \tag{7}$$

and the molar volume of the solution v is given by

$$v = \frac{V}{n_{\mathrm{S}} + n_{\mathrm{W}}} \, . \tag{8}$$

The molar volumes $v(x_{\mathrm{S}})$ are accessible from the experimental density data in Table 3. By rescaling to an arbitrary number for n_{W}, which is held constant, a plot of $V(n_{\mathrm{S}})$ can be generated. From that plot and Eq. (8) the overall partial molar volume of the salt in the aqueous solution v_{S} can be obtained. Here, the dependence of V on n_{S} at constant n_{W} is linear in the investigated concentration range and hence the overall partial molar volume of the alkali halide salts v_{S} in aqueous solution is found to be constant at a given temperature. The experimental overall partial molar volume data for the different alkali halide salt solutions are listed for 293.15 and 333.15 K in Table 10. As the properties introduced in Section 4.1, v_{S} is almost independent on the temperature in the investigated temperature range.

Literature Cited

[1] Washburn, E. *International Critical Tables of Numerical Data, Physics, Chemistry and Technology*; Springer: Hamburg, 2003

[2] Weast, R. *Handbook of Chemistry and Physics*, 68th ed.; CRC Press: Boca Raton, 1987

[3] Lobo, V. M. *Electrolyte solutions: Literature data on thermodynamic and transport properties*; Departmento de Qumica da Universidade de Coimbra, Volume I, 1984

[4] Dortmund Data Bank. **2013**, *Version 2.7.0.46*

[5] DETHERM ORS. **2008**, *Version 2008.6/2.40*

[6] Horvath, A. L. *Handbook of aqueous electrolyte solutions*; Ellis Horwood: Chichester, 1985

[7] Reikhardt, A. General Relations between Composition of Solutions and their Densities. 1. Aqueous Electrolyte Solutions. *Russ. J. Phys. Chem.* **1970**, *44*, 1628–1630

[8] Koptev, G. P. Density of Water in Aqueous-Salt Solutions. *Russ. J. Phys. Chem.* **1977**, *51*, 702–704

[9] Aqvist, J. Ion Water Interaction Potentials Derived From Free-energy Perturbation Simulations. *J. Phys. Chem.* **1990**, *94*, 8021–8024

[10] Dang, L. X. Fluoride-fluoride Association In Water From Molecular-dynamics Simulations. *Chem. Phys. Lett.* **1992**, *200*, 21–25

[11] Dang, L. X. Development of Nonadditive Intermolecular Potentials Using Molecular-dynamics - Solvation of Li+ and F- Ions In Polarizable Water. *J. Chem. Phys.* **1992**, *96*, 6970–6977

[12] Dang, L. X.; Garrett, B. C. Photoelectron-spectra of the Hydrated Iodine Anion From Molecular-dynamics Simulations. *J. Chem. Phys.* **1993**, *99*, 2972–2977

[13] Smith, D. E.; Dang, L. X. Computer-Simulations Of NaCl Association In Polarizable Water. *J. Chem. Phys.* **1994**, *100*, 3757–3766

[14] Dang, L. X. Mechanism and Thermodynamics of Ion Selectivity In Aqueous-solutions of 18-crown-6 Ether - A Molecular-dynamics Study. *J. Am. Chem. Soc.* **1995**, *117*, 6954–6960

[15] Peng, Z. W.; Ewig, C. S.; Hwang, M. J.; Waldman, M.; Hagler, A. T. Derivation of class II force fields .4. van der Waals parameters of alkali metal cations and halide anions. *J. Phys. Chem. A* **1997**, *101*, 7243–7252

[16] Wheeler, D. R.; Newman, J. Molecular dynamics simulations of multicomponent diffusion. 1. Equilibrium method. *J. Phys. Chem. B* **2004**, *108*, 18353–18361

[17] Jensen, K. P.; Jorgensen, W. L. Halide, ammonium, and alkali metal ion parameters for modeling aqueous solutions. *J. Chem. Theory Comput.* **2006**, *2*, 1499–1509

[18] Joung, I. S.; Cheatham, T. E. Determination of alkali and halide monovalent ion parameters for use in explicitly solvated biomolecular simulations. *J. Phys. Chem. B* **2008**, *112*, 9020–9041

[19] Horinek, D.; Mamatkulov, S. I.; Netz, R. R. Rational design of ion force fields based on thermodynamic solvation properties. *J. Chem. Phys.* **2009**, *130*, 124507

[20] Klasczyk, B.; Knecht, V. Kirkwood-Buff derived force field for alkali chlorides in simple point charge water. *J. Chem. Phys.* **2010**, *132*, 024109

[21] Reif, M. M.; Hünenberger, P. H. Computation of methodology-independent single-ion solvation properties from molecular simulations. IV. Optimized Lennard-Jones interaction parameter sets for the alkali and halide ions in water. *J. Chem. Phys.* **2011**, *134*, 144104

[22] Gee, M. B.; Cox, N. R.; Jiao, Y. F.; Bentenitis, N.; Weerasinghe, S.; Smith, P. E. A Kirkwood-Buff Derived Force Field for Aqueous Alkali Halides. *J. Chem. Theory Comput.* **2011**, *7*, 1369–1380

[23] Reiser, S.; Deublein, S.; Vrabec, J.; Hasse, H. Molecular dispersion energy parameters for alkali and halide ions in aqueous solution. *J. Chem. Phys.* **2014**, *140*, 044504

[24] Moucka, F.; Nezbeda, I.; Smith, W. R. Molecular force fields for aqueous electrolytes: SPC/E-compatible charged LJ sphere models and their limitations. *J. Chem. Phys.* **2013**, *138*, 154102

[25] Deublein, S.; Vrabec, J.; Hasse, H. A set of molecular models for alkali and halide ions in aqueous solution. *J. Chem. Phys.* **2012**, *136*, 084501

[26] Berendsen, H. J. C.; Grigera, J. R.; Straatsma, T. P. The Missing Term In Effective Pair Potentials. *J. Phys. Chem.* **1987**, *91*, 6269–6271

[27] Impey, R. W.; Madden, P. A.; McDonald, I. R. Hydration And Mobility of Ions in Solution. *J. Phys. Chem.* **1983**, *87*, 5071–5083

[28] Reddy, M.; Berkowitz, M. Temperature Dependence of Conductance of the Li+, Cs+, and Cl- Ions in Water: Molecular Dynamics Simulation. *J. Chem. Phys.* **1988**, *88*, 7104–7110

[29] Egorov, A.; Komolkin, A.; Chizhik, V.; Yushmanov, P.; Lyubartsev, A.; Laaksonen, A. Temperature and concentration effects on Li+-ion hydration. A molecular dynamics simulation study. *J. Phys. Chem. B* **2003**, *107*, 3234–3242

[30] Zavitsas, A. Aqueous solutions of calcium ions: Hydration numbers and the effect of temperature. *J. Phys. Chem. B* **2005**, *109*, 20636–20640

[31] Bastug, T.; Kuyucak, S. Temperature dependence of the transport coefficients of ions from molecular dynamics simulations. *Chem. Phys. Lett.* **2005**, *408*, 84–88

[32] Ponder, J. W.; Case, D. A. Force fields for protein simulations. *Adv. Protein Chem.* **2003**, *66*, 27–85

[33] Brooks, B. R.; Brooks, C. L., III; Mackerell, A. D., Jr.; Nilsson, L.; Petrella, R. J.; Roux, B.; Won, Y.; Archontis, G.; Bartels, C.; Boresch, S.; Caflisch, A.; Caves, L.; Cui, Q.; Dinner, A. R.; Feig, M.; Fischer, S.; Gao, J.; Hodoscek, M. Im, W.; Kuczera, K.; Lazaridis, T.; Ma, J.; Ovchinnikov, V.; Paci, E.; Pastor, R. W.; Post, C. B.; Pu, J. Z.; Schaefer, M.; Tidor, B.; Venable, R. M.; Woodcock, H. L.; Wu, X.; Yang, W.; York, D. M.; Karplus, M. *J. Comput. Chem.* **2009**, *30*, 1545–1614.

[34] Christen, M.; Hunenberger, P. H.; Bakowies, D.; Baron, R.; Burgi, R.; Geerke, D. P.; Heinz, T. N.; Kastenholz, M. A.; Krautler, V.; Oostenbrink, C.; Peter, C.; Trzesniak, D.; Van Gunsteren, W. F. The GROMOS software for biomolecular simulation: GROMOS05. *J. Comput. Chem.* **2005**, *26*, 1719–1751

[35] Lorentz, H. Über die Anwendung des Satzes vom Virial in der kinetischen Theorie der Gase. *Ann. Phys. (Berlin, Ger.)* **1881**, *248*, 127–136

[36] Berthelot, D. Sur le mlange des gaz. *C. R. Acad. Sci.* **1898**, *126*, 1703–1706

[37] Schnabel, T.; Vrabec, J.; Hasse, H. Unlike Lennard-Jones parameters for vapor-liquid equilibria. *J. Mol. Liq.* **2007**, *135*, 170–178

[38] Allen, M.; Tildesley, D. *Computer Simulation of Liquids*; Clarendon Press: Oxford, 1987

[39] Robinson, R. A.; Stokes, R. H. *Electrolyte Solutions*, 2nd ed.; Butterworth: London, 1955

[40] Koneshan, S.; Rasaiah, J. C.; Lynden-Bell, R. M.; Lee, S. H. Solvent structure, dynamics, and ion mobility in aqueous solutions at 25 degrees C. *J. Phys. Chem. B* **1998**, *102*, 4193–4204

[41] Green, M. Markoff Random Processes and the Statistical Mechanics of Time-Dependent Phenomena.2. Irreversible Processes in Fluids. *J. Chem. Phys.* **1954**, *22*, 398–413

[42] Kubo, R. Statistical-Mechanical Theory of Irreversible Processes .1. General Theory and Simple Applications to Magnetic and Conduction Problems. *J. Phys. Soc. Jpn.* **1957**, *12*, 570–586

[43] Gubbins, K. *Statistical Mechanics Vol. 1*; The Chemical Society Burlington House: London, 1972

[44] Del Popolo, M. G.; Voth, G. A. On the Structure and Dynamics of Ionic Liquids. *J. Phys. Chem. B* **2004**, *108*, 1744–1752

[45] Deublein, S.; Eckl, B.; Stoll, J.; Lishchuk, S. V.; Guevara-Carrion, G.; Glass, C. W.; Merker, T.; Bernreuther, M.; Hasse, H.; Vrabec, J. ms2: A molecular simulation tool for thermodynamic properties. *Comput. Phys. Commun.* **2011**, *182*, 2350–2367

[46] Mähler, J.; Persson, I. A Study of the Hydration of the Alkali Metal Ions in Aqueous Solution. *Inorg. Chem.* **2012**, *51*, 425–438

[47] Dullien, F. A. L. Predictive Equations For Self-Diffusion in Liquids - Different Approach. *AIChE J.* **1972**, *18*, 62–70

[48] Gillen, K.; Douglass, D.; Hoch, J. Self-Diffusion in Liquids Water tool -31 Degrees C. *J. Chem. Phys.* **1972**, *57*, 5117–5119

[49] Mills, R. Self-Diffusion in Normal and Heavy-Wwater in Range 1-45 Degrees. *J. Phys. Chem.* **1973**, *77*, 685–688

[50] Harris, K.; Woolf, L. Pressure and Temperature-Dependence of the Self-Diffusion Coefficient of Water and O-18 Water. *J. Chem. Soc., Faraday Trans. 1* **1980**, *76*, 377–385

[51] Easteal, A.; Price, W.; Woolf, L. Diaphragm Cell for High-Temperature Diffusion Measurements - Tracer Diffusion-Coefficients for Water to 363 K. *J. Chem. Soc., Faraday Trans. 1* **1989**, *85*, 1091–1097

[52] Holz, M.; Heil, S.; Sacco, A. Temperature-dependent self-diffusion coefficients of water and six selected molecular liquids for calibration in accurate H-1 NMR PFG measurements. *Phys. Chem. Chem. Phys.* **2000**, *2*, 4740–4742

[53] Guevara-Carrion, G.; Vrabec, J.; Hasse, H. Prediction of self-diffusion coefficient and shear viscosity of water and its binary mixtures with methanol and ethanol by molecular simulation. *J. Chem. Phys.* **2011**, *134*, 074508

[54] Mills, R.; Lobo, V. *Self-diffusion in electrolyte solutions*; Elsevier: New York, 1989

[55] Lee, S. H.; Rasaiah, J. C. Molecular-Dynamics Simulation of Ionic Mobility .1. Alkali-Metal Cations In Water At 25-Degrees-C. *J. Chem. Phys.* **1994**, *101*, 6964–6974

[56] Lee, S. H.; Rasaiah, J. C. Molecular dynamics simulation of ion mobility .2. Alkali metal and halide ions using the SPC/E model for water at 25 degrees C. *J. Phys. Chem.* **1996**, *100*, 1420–1425

[57] Flyvbjerg, H.; Petersen, H. G. Error-Estimates On Averages of Correlated Data. *J. Chem. Phys.* **1989**, *91*, 461–466

[58] Ewald, P. P. Die Berechnung optischer und elektrostatischer Gitterpotenziale. *Ann. Phys. (Berlin, Ger.)* **1921**, *369*, 253–287

[59] Hansen, J. P.; McDonald, I. *Theory of Simple Liquids*; Academic Press: Amsterdam, 1986

[60] Wagner, W.; Pruss, A. The IAPWS Formulation 1995 for the Thermodynamic Properties of Ordinary Water Substance for General and Scientific Use. *J. Phys. Chem. Ref. Data* **2002**, *31*, 387–535

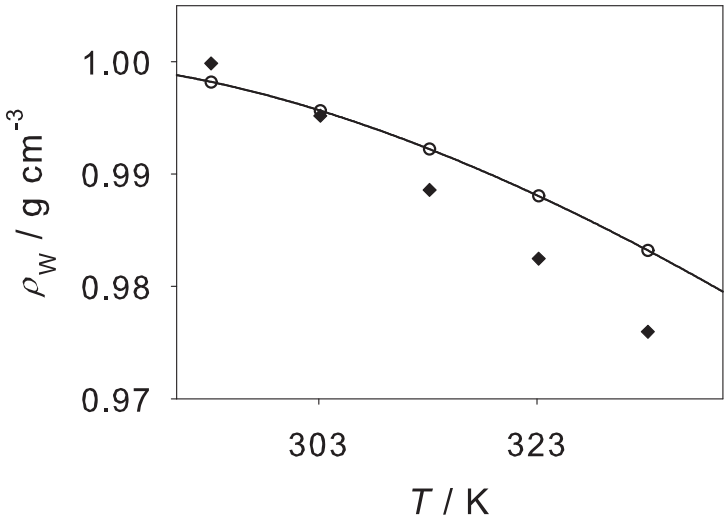

Figure 1: Density of pure liquid water as a function of temperature at 1 bar. Results of simulations from the present work with the SPC/E model[26] (◆) are compared to experimental data from the present work (○). The line indicates a correlation of experimental data from the literature.[60]

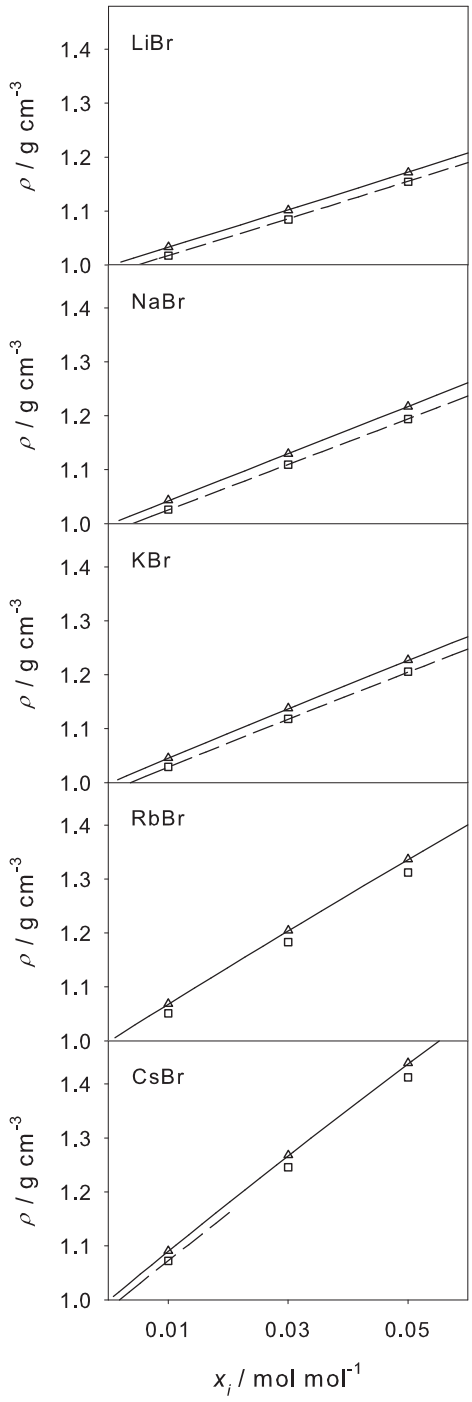

Figure 2: Density of aqueous lithium, sodium, potassium, rubidium and cesium bromide salt solutions as a function of the ion mole fraction at 1 bar. Present experimental data (symbols) are compared to correlations of literature data[1–3] (lines): 293.15 K (△, —) and 333.15 K (□, - - -).

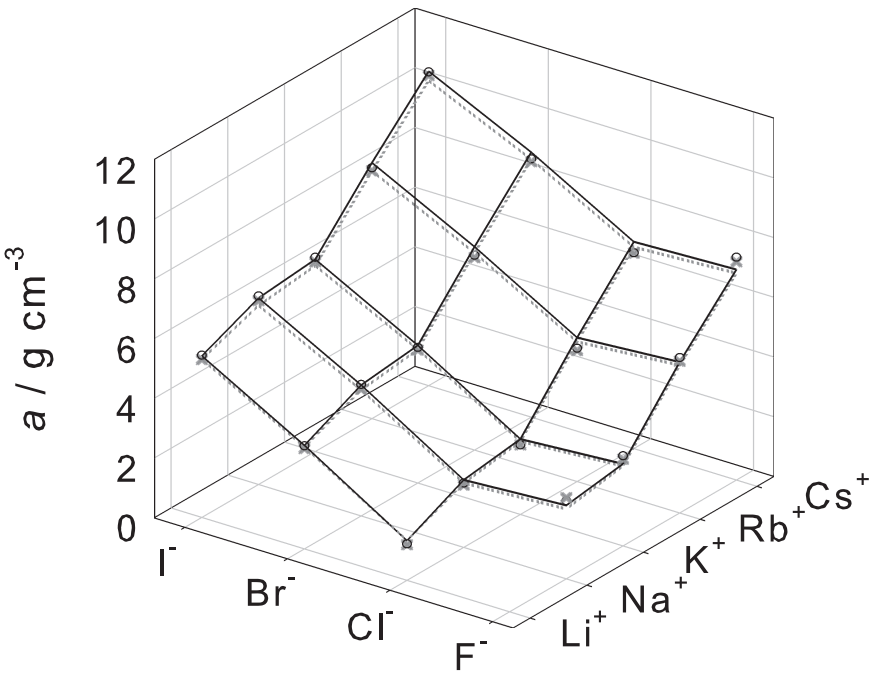

Figure 3: Slope of the density of aqueous alkali halide salt solutions over the ion mole fraction at 1 bar. Present simulation data (symbols) are compared to present experimental data (lines): 293.15 K (∘, —) and 333.15 K (×, ···). For several solutions the lines and symbols of the different temperatures lie upon each other.

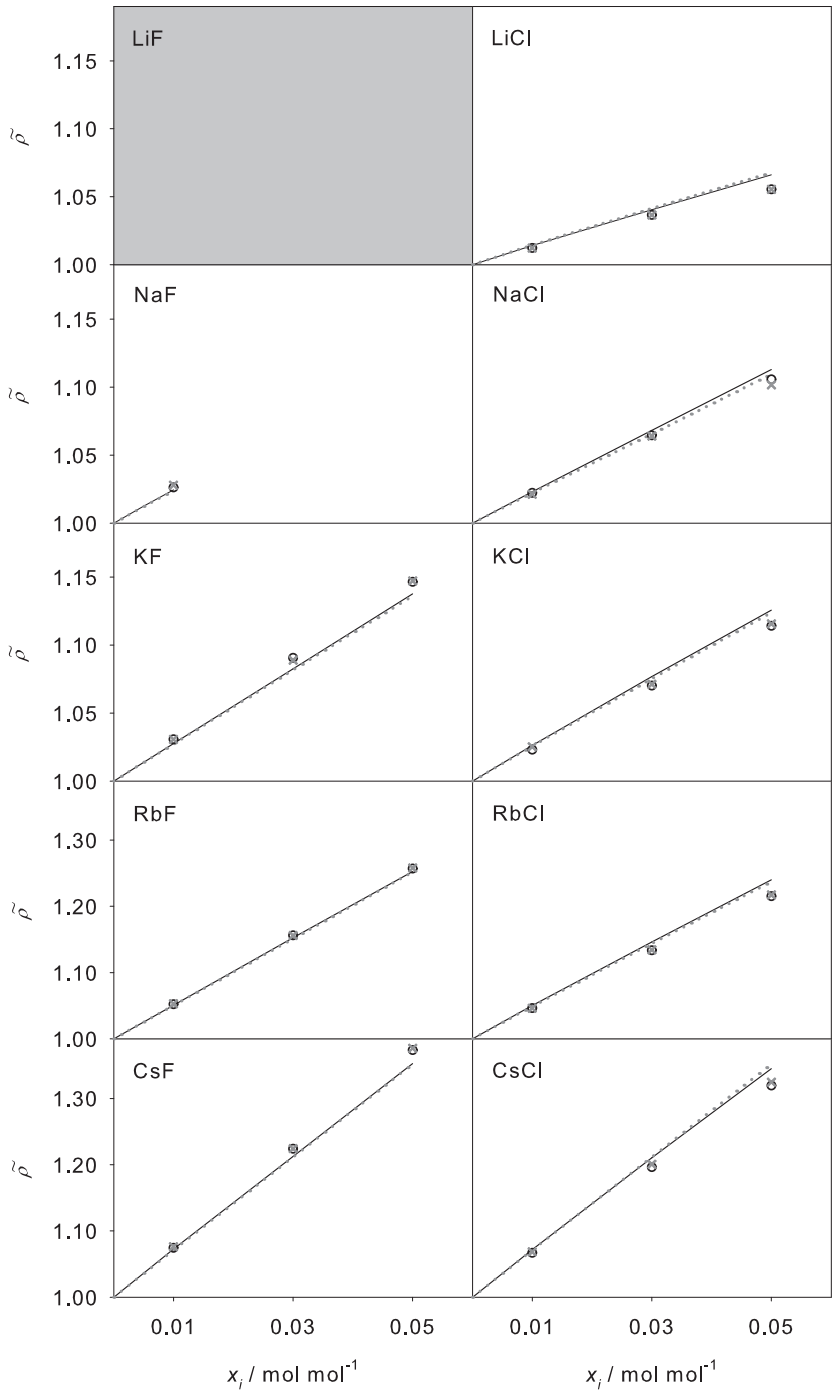

Figure 4: Reduced density of aqueous alkali fluoride and chloride salt solutions as a function of the ion mole fraction at 1 bar. Present simulation data (symbols) are compared to correlations of the present experimental data (lines): 293.15 K (○, —) and 333.15 K (×, ···). For several solutions the lines and symbols of the different temperatures lie upon each other. LiF is only soluble in trace amounts and hence no data are shown here.

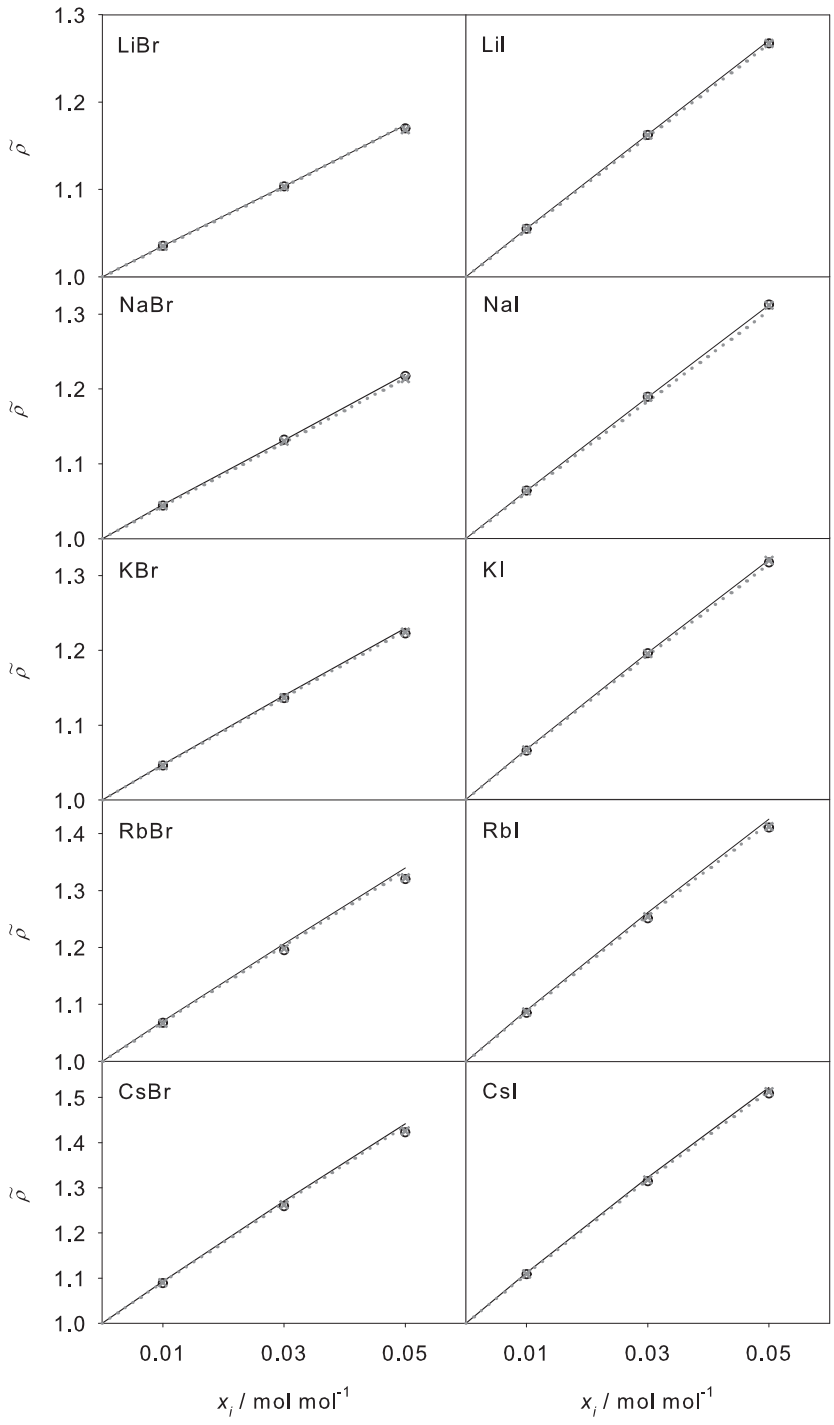

Figure 5: Reduced density of aqueous alkali bromide and iodide salt solutions as a function of the ion mole fraction at 1 bar. Present simulation data (symbols) are compared to correlations of the present experimental data (lines): 293.15 K (∘, —) and 333.15 K (×, ···). For several solutions the lines and symbols of the different temperatures lie upon each other.

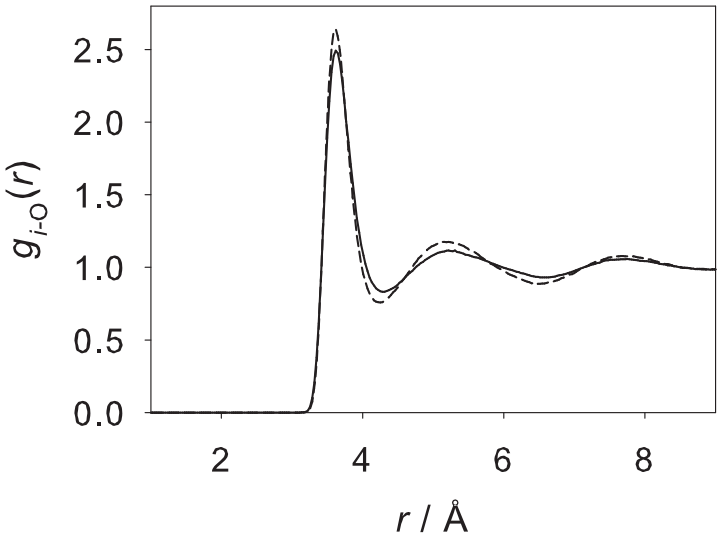

Figure 6: Radial distribution function of SPC/E water[26] around I^- for 293.15 K (- - -) and 333.15 K (—) at 1 bar. The position of water was represented by the position of the oxygen atom.

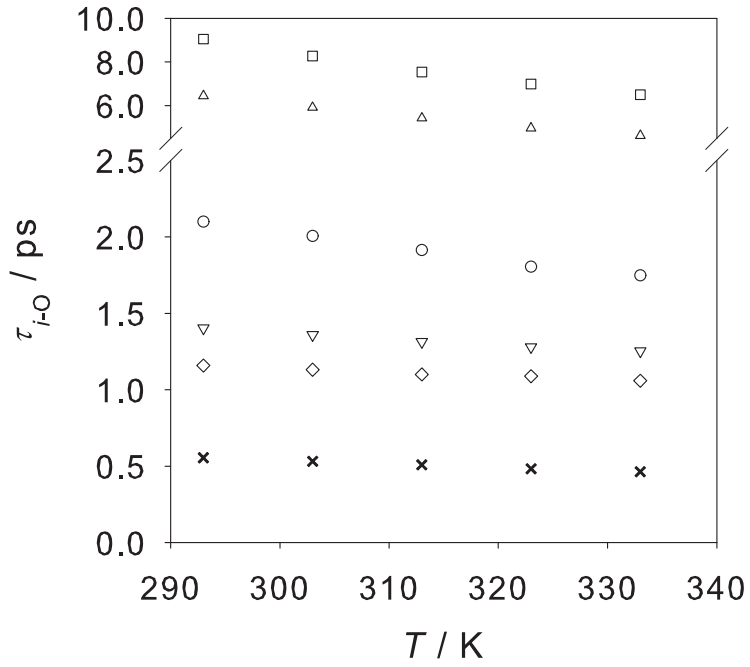

Figure 7: Residence time of SPC/E water[26] around alkali cations Li^+(□), Na^+(△), K^+(○), Rb^+(▽), Cs^+(◇) in aqueous solution (x_i = 0.01 mol/mol) and its residence time around another neighboring molecule for pure liquid water (×) as a function of the temperature at 1 bar.

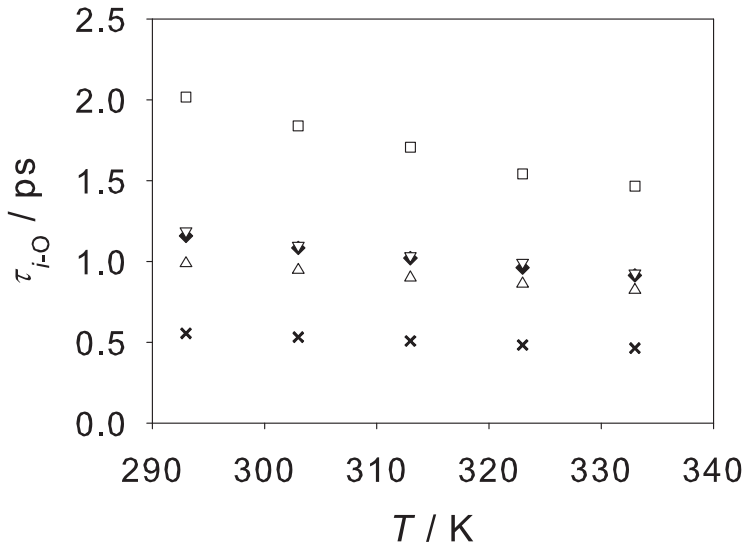

Figure 8: Residence time of SPC/E water[26] around alkali anions F^-(□), Cl^-(▽), Br^-(◆), I^-(△) in aqueous solution (x_i = 0.01 mol/mol) and its residence time around another neighboring molecule for pure liquid water (×) as a function of the temperature at 1 bar.

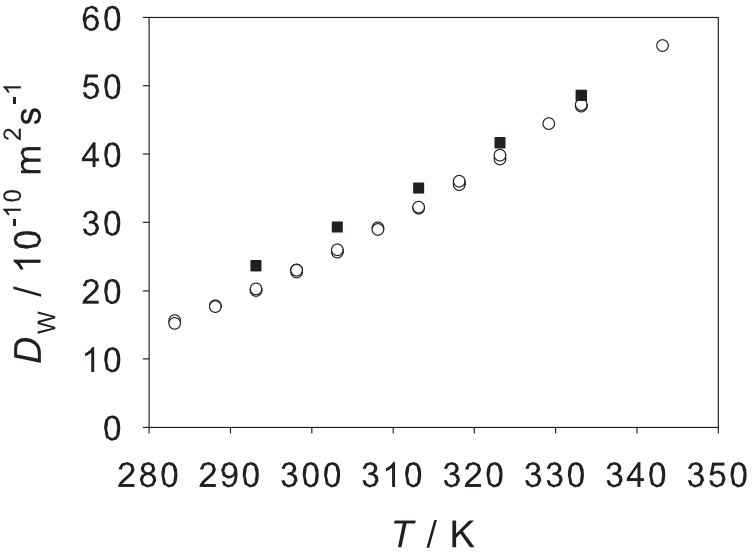

Figure 9: Self-diffusion coefficient of pure liquid water as a function of temperature at 1 bar. Present simulation results with SPC/E water[26] (■) are compared to experimental data (○)[47–52]

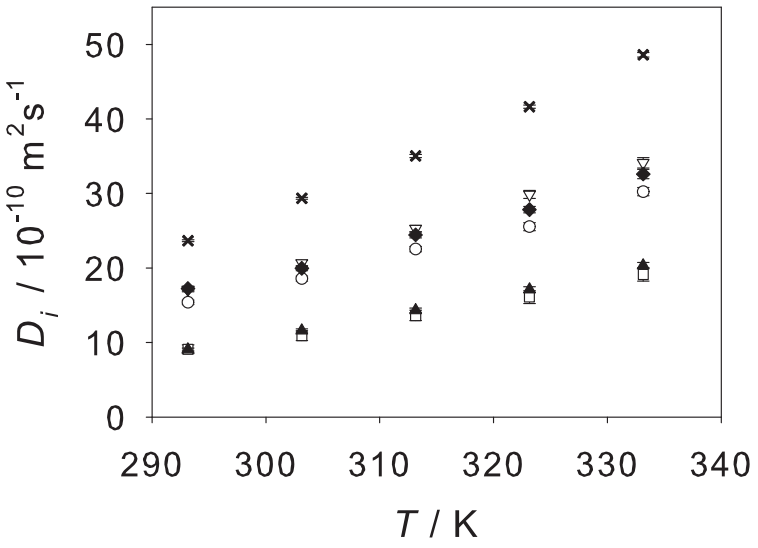

Figure 10: Self-diffusion coefficient of alkali cations Li^+(□), Na^+(▲), K^+(○), Rb^+(▽), Cs^+(♦) in aqueous solution (x_i = 0.009 mol/mol) and of pure liquid SPC/E water[26] (×) as a function of temperature at 1 bar. The statistical simulation uncertainties of the self-diffusion coefficients of the alkali cations are below $\pm 0.9 \cdot 10^{-10}$ and of water below $\pm 0.3 \cdot 10^{-10}$ m^2s^{-1}.

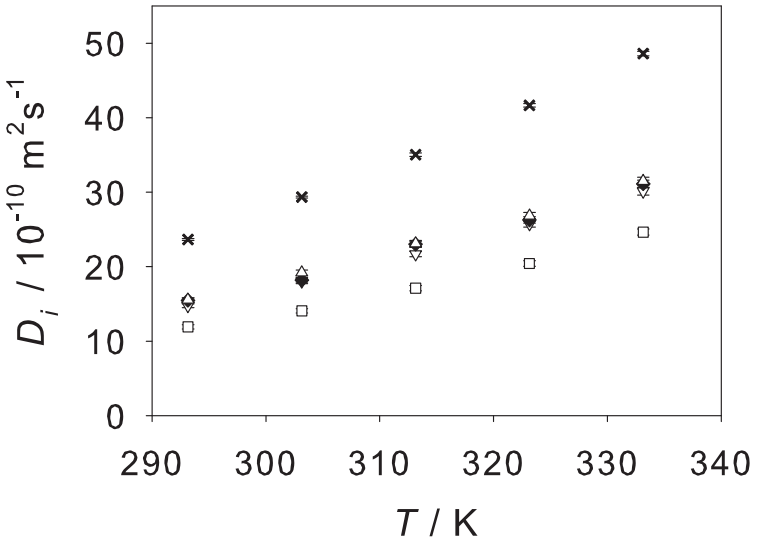

Figure 11: Self-diffusion coefficient of halide anions F^-(□), Cl^-(▽), Br^-(♦), I^-(△) in aqueous solution (x_i = 0.009 mol/mol) and of pure liquid SPC/E water[26] (×) as a function of the temperature at 1 bar. The statistical simulation uncertainties of the self-diffusion coefficients of the halide anions are below $\pm 0.6 \cdot 10^{-10}$ and of water below $\pm 0.3 \cdot 10^{-10}$ m^2s^{-1}.

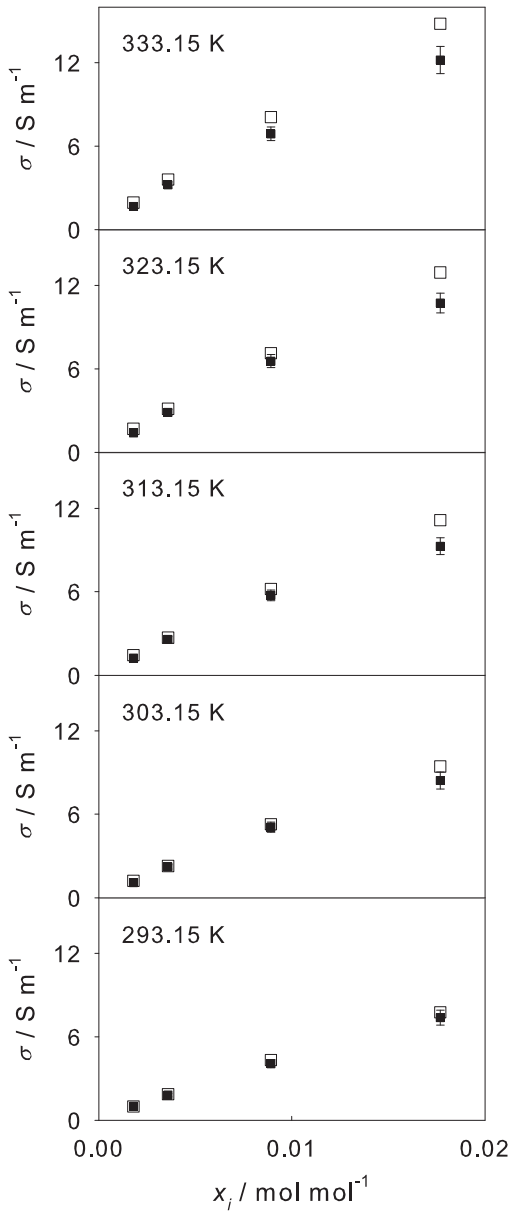

Figure 12: Electric conductivity of aqueous NaCl salt solutions as a function of the ion mole fraction at 1 bar. Simulation results (■) are compared to experimental data[3] (□). The statistical simulation uncertainties of the electric conductivities are found to be about ±8% for all investigated concentrations at all temperatures.

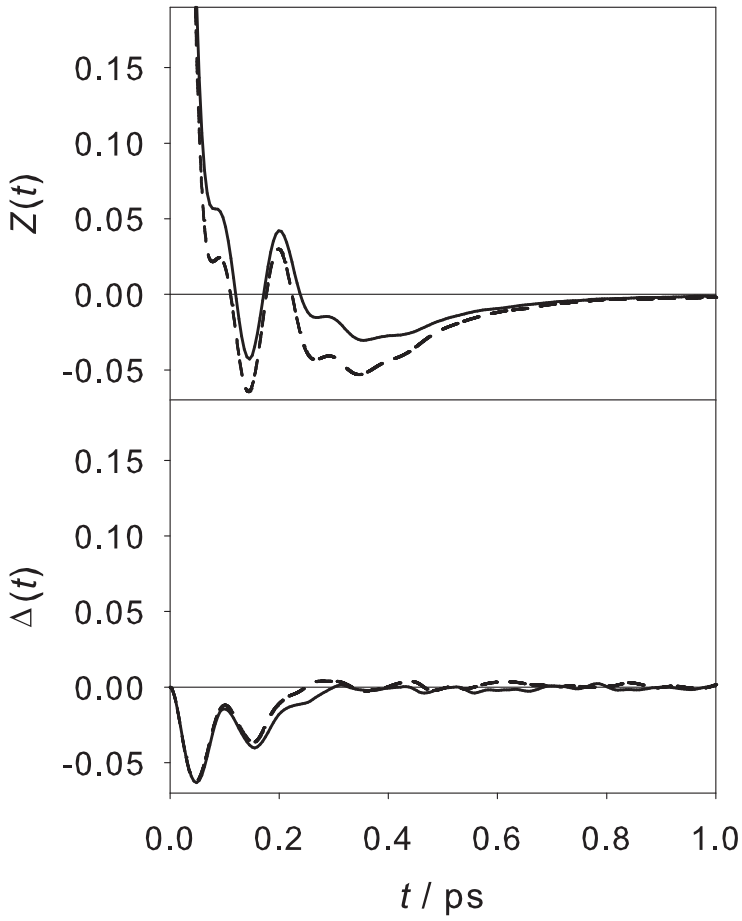

Figure 13: Electric current time correlation function of the aqueous NaCl salt solution (x_i = 0.018 mol/mol) separated into its autocorrelation function $Z(t)$ (top) and crosscorrelation function $\Delta(t)$ (bottom) at 293.15 K (- - -) and 333.15 K (—) at 1 bar .

Table 1: Purity and supplier of the alkali halide salts

salt	purity	supplier
LiCl	≥ 99 %	Merck
LiBr	≥ 99.999 %	Roth
LiI	≥ 99 %	AlfaAesar
NaF	≥ 99 %	Merck
NaCl	≥ 99.5 %	Merck
NaBr	≥ 99 %	Merck
NaI	≥ 99.5 %	Merck
KF	≥ 99 %	Merck
KCl	≥ 99.5 %	Merck
KBr	≥ 99.5 %	Merck
KI	≥ 99 %	Fluka
RbF	≥ 99.8 %	Aldrich
RbCl	≥ 99.8 %	Aldrich
RbBr	≥ 99.7 %	Aldrich
RbI	≥ 99.8 %	AlfaAesar
CsF	≥ 99.9 %	Aldrich
CsCl	≥ 99.999 %	Roth
CsBr	≥ 99.5 %	Fluka
CsI	≥ 99.999 %	Aldrich

Table 2: LJ size parameter σ and LJ energy parameter ε for alkali and halide ions. The parameters were taken from preceding work.[23,25]

Ion	σ / Å	ε/k_B / K
Li^+	1.88	200
Na^+	1.89	200
K^+	2.77	200
Rb^+	3.26	200
Cs^+	3.58	200
F^-	3.66	200
Cl^-	4.41	200
Br^-	4.54	200
I^-	4.78	200

Table 3: Experimental data of the density ρ of aqueous alkali halide salt solutions at 1 bar. The overall relative error in x_i is estimated to be below ±0.1%. The accuracy of the density and temperature measurements are found to be better than ±0.0001 g/cm^3 and ±0.1 K, respectively.

T / K	293.15			303.15			313.15			323.15			333.15		
x_i / mol mol^{-1}	0.01	0.03	0.05	0.01	0.03	0.05	0.01	0.03	0.05	0.01	0.03	0.05	0.01	0.03	0.05
Salt	ρ / g cm^{-3}			ρ / g cm^{-3}			ρ / g cm^{-3}			ρ / g cm^{-3}			ρ / g cm^{-3}		
LiCl	1.0123	1.0385	1.0641	1.0097	1.0357	1.0612	1.0062	1.0323	1.0579	1.0021	1.0283	1.0540	0.9974	1.0238	1.0498
LiBr	1.0335	1.1018	1.1715	1.0302	1.0980	1.1680	1.0263	1.0939	1.1639	1.0220	1.0894	1.1593	1.0172	1.0846	1.1543
LiI	1.0533	1.1608	1.2681	1.0498	1.1563	1.2627	1.0457	1.1510	1.2572	1.0412	1.1461	1.2514	1.0362	1.1407	1.2455
NaF	1.0227	–	–	1.0197	–	–	1.0160	–	–	1.0115	–	–	1.0065	–	–
NaCl	1.0213	1.0662	1.1108	1.0183	1.0624	1.1062	1.0145	1.0580	1.1016	1.0101	1.0524	1.0964	1.0051	1.0476	1.0909
NaBr	1.0436	1.1295	1.2171	1.0400	1.1252	1.2118	1.0358	1.1204	1.2062	1.0311	1.1151	1.2002	1.0260	1.1094	1.1940
NaI	1.0617	1.1867	1.3095	1.0584	1.1818	1.3032	1.0542	1.1763	1.2965	1.0495	1.1691	1.2895	1.0441	1.1634	1.2822
KF	1.0257	1.0805	1.1355	1.0228	1.0770	1.1307	1.0192	1.0729	1.1265	1.0148	1.0684	1.1219	1.0100	1.0635	1.1169
KCl	1.0243	1.0748	1.1236	1.0214	1.0712	1.1196	1.0177	1.0670	1.1151	1.0133	1.0624	1.1102	1.0084	1.0572	1.1049
KBr	1.0457	1.1377	1.2274	1.0426	1.1337	1.2226	1.0387	1.1291	1.2174	1.0342	1.1239	1.2117	1.0292	1.1184	1.2057
KI	1.0652	1.1940	1.3179	1.0619	1.1893	1.3121	1.0579	1.1841	1.3060	1.0532	1.1784	1.2993	1.0479	1.1723	1.2924
RbF	1.0487	1.1506	1.2503	1.0457	1.1465	1.2461	1.0420	1.1419	1.2414	1.0376	1.1370	1.2362	1.0326	1.1316	1.2306
RbCl	1.0483	1.1442	1.2379	1.0448	1.1398	1.2328	1.0407	1.1350	1.2275	1.0361	1.1300	1.2220	1.0312	1.1247	1.2163
RbBr	1.0686	1.2046	1.3369	1.0650	1.1997	1.3310	1.0607	1.1945	1.3249	1.0560	1.1889	1.3186	1.0509	1.1829	1.3122
RbI	1.0881	1.2597	1.4232	1.0842	1.2542	1.4163	1.0798	1.2484	1.4092	1.0749	1.2423	1.4020	1.0696	1.2359	1.3946
CsF	1.0709	1.2101	1.3499	1.0680	1.2062	1.3454	1.0643	1.2017	1.3404	1.0599	1.1966	1.3349	1.0530	1.1909	1.3291
CsCl	1.0699	1.2083	1.3426	1.0663	1.2036	1.3370	1.0621	1.1986	1.3312	1.0575	1.1932	1.3252	1.0524	1.1877	1.3191
CsBr	1.0905	1.2679	1.4388	1.0867	1.2628	1.4326	1.0823	1.2573	1.4260	1.0776	1.2515	1.4193	1.0724	1.2455	1.4124
CsI	1.1095	1.3207	1.5194	1.1056	1.3149	1.5121	1.1010	1.3089	1.5045	1.0960	1.3025	1.4969	1.0906	1.2959	1.4891
Water	0.9982			0.9957			0.9922			0.9881			0.9832		

Table 4: Slope a of the density ρ of aqueous alkali halide solutions over the ion mole fraction x_i at 1 bar. For all lithium, sodium and potassium halide salts the standard deviation of the correlation for the density of the aqueous electrolyte solutions (Eq. (5)) is better than ±0.001 g/cm^3 and for the rubidium and cesium halide salts better than ±0.003 g/cm^3. Exceptional cases are the solutions of KI with a standard deviation of ±0.003 g/cm^3, of RbI with ±0.004 g/cm^3 and of CsI with ±0.006 g/cm^3.

T / K	293.15	333.15		293.15	333.15		293.15	333.15		293.15	333.15		293.15	333.15
Salt	a / g cm^{-3}		Salt	a / g cm^{-3}		Salt	a / g cm^{-3}		Salt	a / g cm^{-3}		Salt	a / g cm^{-3}	
			NaF	2.45	2.34	KF	2.75	2.68	RbF	5.05	4.95	CsF	7.05	6.93
LiCl	1.33	1.34	NaCl	2.26	2.15	KCl	2.52	2.52	RbCl	4.82	4.68	CsCl	6.93	6.74
LiBr	3.46	3.41	NaBr	4.38	4.22	KBr	4.61	4.47	RbBr	6.81	6.61	CsBr	8.87	8.63
LiI	5.41	5.26	NaI	6.24	5.99	KI	6.41	6.22	RbI	8.57	8.29	CsI	10.53	10.21

Table 5: Molecular simulation data for the density ρ of aqueous alkali halide salt solutions at 1 bar. The statistical simulation uncertainties of the densities are throughout below ±0.0005 g/cm^3.

T / K	293.15			303.15			313.15			323.15			333.15		
x_i / mol mol^{-1}	0.01	0.03	0.05	0.01	0.03	0.05	0.01	0.03	0.05	0.01	0.03	0.05	0.01	0.03	0.05
Salt	ρ / g cm^{-3}			ρ / g cm^{-3}			ρ / g cm^{-3}			ρ / g cm^{-3}			ρ / g cm^{-3}		
LiCl	1.0103	1.0316	1.0479	1.0052	1.0247	1.0418	0.9995	1.0190	1.0346	0.9932	1.0122	1.0294	0.9870	1.0058	1.0232
LiBr	1.0317	1.0971	1.1599	1.0275	1.0910	1.1520	1.0205	1.0837	1.1460	1.0128	1.0775	1.1376	1.0073	1.0705	1.1317
LiI	1.0516	1.1568	1.2576	1.0466	1.1500	1.2490	1.0417	1.1430	1.2431	1.0341	1.1358	1.2334	1.0268	1.1286	1.2259
NaF	1.0254	–	–	1.0207	–	–	1.0142	–	–	1.0085	–	–	1.0002	–	–
NaCl	1.0193	1.0589	1.0938	1.0142	1.0518	1.0875	1.0084	1.0460	1.0799	1.0020	1.0390	1.0745	0.9957	1.0325	1.0680
NaBr	1.0406	1.1241	1.2052	1.0364	1.1179	1.1970	1.0293	1.1105	1.1907	1.0216	1.1041	1.1820	1.0160	1.0969	1.1759
NaI	1.0605	1.1834	1.3017	1.0555	1.1764	1.2928	1.0505	1.1693	1.2866	1.0428	1.1619	1.2767	1.0355	1.1545	1.2688
KF	1.0282	1.0808	1.1295	1.0222	1.0752	1.1228	1.0164	1.0709	1.1169	1.0109	1.0633	1.1111	1.0031	1.0563	1.1048
KCl	1.0209	1.0609	1.1015	1.0174	1.0560	1.0956	1.0112	1.0513	1.0891	1.0036	1.0456	1.0829	0.9971	1.0394	1.0763
KBr	1.0431	1.1270	1.2088	1.0375	1.1196	1.2025	1.0320	1.1158	1.1953	1.0263	1.1091	1.1900	1.0180	1.1013	1.1812
KI	1.0628	1.1867	1.3014	1.0593	1.1809	1.2964	1.0516	1.1732	1.2893	1.0449	1.1676	1.2813	1.0381	1.1582	1.2744
RbF	1.0488	1.1441	1.2402	1.0447	1.1372	1.2345	1.0371	1.1334	1.2261	1.0323	1.1264	1.2173	1.0234	1.1192	1.2115
RbCl	1.0432	1.1220	1.2000	1.0354	1.1167	1.1943	1.0321	1.1123	1.1861	1.0254	1.1055	1.1812	1.0172	1.0979	1.1740
RbBr	1.0644	1.1858	1.3029	1.0591	1.1799	1.2952	1.0531	1.1750	1.2895	1.0470	1.1676	1.2823	1.0386	1.1600	1.2750
RbI	1.0836	1.2434	1.3912	1.0789	1.2372	1.3861	1.0723	1.2301	1.3801	1.0648	1.2235	1.3710	1.0590	1.2150	1.3633
CsF	1.0727	1.2153	1.3484	1.0644	1.2042	1.3432	1.0605	1.2014	1.3372	1.0527	1.1918	1.3298	1.0459	1.1847	1.3219
CsCl	1.0643	1.1883	1.3038	1.0598	1.1814	1.2988	1.0542	1.1764	1.2909	1.0464	1.1689	1.2834	1.0398	1.1610	1.2749
CsBr	1.0862	1.2499	1.4035	1.0805	1.2437	1.3964	1.0751	1.2365	1.3904	1.0688	1.2296	1.3830	1.0605	1.2220	1.3748
CsI	1.1059	1.3036	1.4921	1.0987	1.2992	1.4830	1.0934	1.2913	1.4746	1.0873	1.2842	1.4662	1.0793	1.2764	1.4571
Water	0.9999			0.9952			0.9886			0.9825			0.9760		

Table 6: RDF $g_{i-\mathrm{O}}(r)$ of water around the alkali and halide ions i in aqueous solutions (x_i =0.01 mol/mol) at the first maximum $r_{\mathrm{max},1}$, first minimum $r_{\mathrm{min},1}$ and second maximum $r_{\mathrm{max},2}$ at 1 bar.

T / K	293.15	313.15	333.15	293.15	313.15	333.15
Ion	$r_{\mathrm{max},1}$ / Å			$g(r_{\mathrm{max},1})$		
Li^+	2.232	2.232	2.232	9.729	9.436	9.285
Na^+	2.232	2.232	2.232	9.758	9.515	9.318
K^+	2.684	2.684	2.684	5.273	5.161	4.995
Rb^+	2.956	2.956	2.956	3.948	3.867	3.786
Cs^+	3.137	3.137	3.137	3.326	3.233	3.198
F^-	3.016	3.016	3.016	4.896	4.727	4.556
Cl^-	3.408	3.408	3.408	3.227	3.088	3.006
Br^-	3.499	3.499	3.499	3.076	2.968	2.878
I^-	3.619	3.619	3.619	2.640	2.592	2.492
Ion	$r_{\mathrm{min},1}$ / Å			$g(r_{\mathrm{min},1})$		
Li^+	3.076	3.076	3.107	0.072	0.086	0.105
Na^+	3.076	3.076	3.076	0.072	0.087	0.103
K^+	3.468	3.468	3.529	0.418	0.437	0.454
Rb^+	3.830	3.861	3.861	0.631	0.644	0.652
Cs^+	4.011	4.102	4.132	0.767	0.757	0.766
F^-	3.649	3.680	3.710	0.365	0.408	0.461
Cl^-	4.041	4.041	4.102	0.590	0.650	0.691
Br^-	4.102	4.222	4.162	0.648	0.698	0.732
I^-	4.222	4.283	4.283	0.757	0.791	0.832
Ion	$r_{\mathrm{max},2}$ / Å			$g(r_{\mathrm{max},2})$		
Li^+	4.403	4.403	4.434	1.535	1.496	1.455
Na^+	4.373	4.403	4.403	1.542	4.403	1.471
K^+	4.765	4.765	4.826	1.206	1.199	1.169
Rb^+	4.976	5.037	5.097	1.072	1.067	1.061
Cs^+	5.218	5.308	5.459	1.004	0.996	0.995
F^-	4.795	4.856	4.856	1.301	1.262	1.223
Cl^-	5.097	5.097	5.097	1.214	1.167	1.136
Br^-	5.157	5.157	5.157	1.203	1.177	1.142
I^-	5.218	5.188	5.218	1.176	1.146	1.116

Table 7: Hydration number $n_{i-\mathrm{O}}$ in the first hydration shell around the alkali and halide ions i in aqueous solutions (x_i =0.01 mol/mol) at 1 bar. The statistical simulation uncertainty was throughout ±0.2.

T / K	293.15	313.15	333.15
Ion	$n_{i-\mathrm{O}}$		
Li^+	5.5	5.3	5.3
Na^+	5.4	5.3	5.3
K^+	6.4	6.3	6.3
Rb^+	7.3	7.2	7.4
Cs^+	7.9	8.2	8.2
F^-	6.9	6.9	6.8
Cl^-	6.9	7.2	7.1
Br^-	7.6	7.5	7.7
I^-	7.5	7.5	7.6

Table 8: Residence time of water molecules in the first hydration shell around ions i ($\tau_{i-\mathrm{O}}$) in aqueous electrolyte solutions (x_i=0.01 mol/mol) and around neighboring water molecules in pure liquid water ($\tau_{\mathrm{O}-\mathrm{O}}$) at 1 bar.

T / K	293.15	303.15	313.15	323.15	333.15
Ion	$\tau_{i-\mathrm{O}}$ / ps				
Li^+	9.05	8.27	7.54	6.99	6.50
Na^+	6.45	5.91	5.42	4.97	4.62
K^+	2.10	2.01	1.91	1.80	1.75
Rb^+	1.40	1.36	1.31	1.28	1.25
Cs^+	1.16	1.13	1.10	1.09	1.06
F^-	2.02	1.84	1.71	1.54	1.47
Cl^-	1.19	1.10	1.03	0.99	0.93
Br^-	1.16	1.08	1.02	0.96	0.91
I^-	0.99	0.95	0.90	0.86	0.82
O	0.55	0.53	0.51	0.48	0.46

Table 9: Self-diffusion coefficient D_i of the alkali cations and halide anions i in aqueous solution (x_i = 0.009 mol/mol) and D_{W} of pure liquid SPC/E water[26] at 1 bar. The number in parentheses indicates the statistical simulation uncertainty in the last digit.

T / K	293.15	303.15	313.15	323.15	333.15
Ion	D_i / 10^{-10} m^{2}s^{-1}				
Li^+	9.1(6)	10.9(7)	13.6(7)	16.1(9)	19.1(9)
Na^+	9.1(2)	11.6(2)	14.3(3)	17.1(4)	20.4(4)
K^+	15.4(3)	18.6(4)	22.5(4)	25.6(5)	30.2(6)
Rb^+	17.1(3)	20.6(4)	25.3(4)	29.9(5)	34.1(7)
Cs^+	17.2(3)	20.0(3)	24.4(4)	27.8(4)	32.6(4)
F^-	11.9(3)	14.1(3)	17.1(4)	20.4(4)	24.6(4)
Cl^-	14.8(3)	18.0(3)	21.7(4)	25.7(4)	30.1(5)
Br^-	15.5(3)	18.2(4)	23.0(4)	26.3(4)	31.1(5)
I^-	15.6(3)	19.6(4)	23.1(4)	26.8(4)	31.5(5)
Water	23.7(1)	29.3(1)	35.0(2)	41.6(2)	48.6(3)

Table 10: Overall partial molar volume of the alkali halide salts v_S in aqueous solution at 1 bar. The standard deviation of the volume of the electrolyte solution (Eq. (6)) is for alkali halide salts throughout below ±0.1%.

T / K	293.15	333.15		293.15	333.15		293.15	333.15		293.15	333.15		293.15	333.15
Salt	v_S / cm^3 mol^{-1}		Salt	v_S / cm^3 mol^{-1}		Salt	v_S / cm^3 mol^{-1}		Salt	v_S / cm^3 mol^{-1}		Salt	v_S / cm^3 mol^{-1}	
			NaF	1.0	1.3	KF	13.9	13.6	RbF	19.3	19.8	CsF	29.8	29.6
LiCl	20.3	20.1	NaCl	20.3	21.5	KCl	30.7	31.6	RbCl	35.7	36.8	CsCl	42.9	44.1
LiBr	26.6	26.6	NaBr	27.2	28.6	KBr	37.0	38.4	RbBr	42.2	43.8	CsBr	49.2	50.9
LiI	36.9	38.2	NaI	37.7	40.3	KI	47.8	50.0	RbI	53.0	55.4	CsI	60.3	62.8

Figure 14: For Table of Contents use only

Title: Temperature dependence of the density of aqueous alkali halide salt solutions by experiment and molecular simulation
Authors: S. Reiser, M. Horsch, H. Hasse